Volume 13. No 2, May 2026
e-ISSN 2527-9572 / p-ISSN 2354-8924

Assessment of AEKF SoC Estimation in a $LiFePO_4$ Battery System with Relay Switching Control

Imam Hidayat Usman
Electrical Engineering Department,
Universitas Andalas.
Jl. Limau Manis, Kelurahan Limau Manis,
Kecamatan Pauh, Kota Padang,
Sumatera Barat, Kode Pos 25163
imam.dayat87@gmail.com

Syafii
Electrical Engineering Department,
Universitas Andalas.
Jl. Limau Manis, Kelurahan Limau Manis,
Kecamatan Pauh, Kota Padang,
Sumatera Barat, Kode Pos 25163
syafii@eng.unand.ac.id

Novizon*
Electrical Engineering Department,
Universitas Andalas.
Jl. Limau Manis, Kelurahan Limau Manis,
Kecamatan Pauh, Kota Padang,
Sumatera Barat, Kode Pos 25163
novizon@eng.unand.ac.id

Aulia
Electrical Engineering Department,
Universitas Andalas
Jl. Limau Manis, Kelurahan Limau Manis,
Kecamatan Pauh, Kota Padang,
Sumatera Barat, Kode Pos 25163
aulia@eng.unand.ac.id

Article history: Received December 24, 2025| Revised February 22, 2026| Accepted April 18, 2026

Abstract **–This study implements an Adaptive Extended Kalman Filter (AEKF) for real-time state of charge (SoC) estimation to support charge–discharge regulation in a $LiFePO_4$ battery system integrated with photovoltaic (PV) generation. Due to the variability of PV output, accurate and stable SoC estimation is essential for ensuring reliable battery operation. A first-order equivalent circuit model (1RC ECM) is employed to represent battery dynamics based on measured current and terminal voltage. The proposed AEKF algorithm is implemented on a Raspberry Pi 5 to enable real-time computation, and the estimated SoC is directly used as the control variable in a dual-relay switching mechanism to regulate charging and discharging processes. Experimental results show that the proposed method achieves a Mean Absolute Error (MAE) of 1.24% and a Root Mean Square Error (RMSE) of 1.58%, which are both below the 5% target specified in the system design. The system successfully maintains the battery within a safe SoC range of 57.5% to 85.2%, while ensuring stable relay operation without chattering under dynamic load and charging conditions. These results demonstrate that the proposed AEKF-based approach provides accurate, stable, and practical SoC estimation, making it suitable for real-time battery management in small-scale energy storage applications.**

Keywords: Adaptive Extended Kalman Filter; State of Charge estimation; LiFePO4 battery, Equivalent circuit model dan Relay switching control.

I. INTRODUCTION

The adoption of renewable energy, particularly solar photovoltaic (PV) generation, has grown steadily as it offers a practical route to reducing reliance on fossil-based sources. However, the stochastic nature of PV output, driven by weather variability, necessitates reliable energy storage systems to buffer the mismatch between generation and load demand. In these systems, a Battery Management System (BMS) is vital for ensuring operational safety and longevity. A core function of the BMS is the accurate estimation of the State of Charge (SoC), which represents the remaining available energy. Inaccurate SoC estimation can lead to suboptimal control decisions, pushing batteries toward accelerated degradation through overcharge or deep discharge [1].

Although SoC cannot be measured directly, it can be estimated using several methods. Conventional approaches such as Coulomb Counting (CC) and Open-Circuit Voltage (OCV) mapping are widely used due to their simplicity. However, these methods suffer from cumulative integration errors and require long relaxation periods for accurate voltage measurement [2], [3]. To overcome these limitations, model-based approaches using the Equivalent Circuit Model (ECM) have been widely adopted due to their balance between computational efficiency and accuracy [4]. Among these approaches, the Extended Kalman Filter (EKF) is widely used for nonlinear SoC estimation because it combines model predictions with measurement data under uncertainty [5]. However, EKF performance is highly dependent on the tuning of process noise covariance (Q) and measurement noise covariance (R). In real-world applications, mismatched Q and R values can lead to estimation errors or divergence [6]. To address this issue, Adaptive Extended Kalman Filter (AEKF) methods

have been proposed to update noise covariance dynamically and improve estimation robustness [7].

In addition, machine learning and data-driven approaches have shown promising results for SoC estimation, achieving high accuracy under controlled conditions. However, these methods generally require large datasets and high computational resources, making them less suitable for low-cost embedded systems [8],[9]. Furthermore, SoC estimation becomes more challenging in Lithium Iron Phosphate ($LiFePO_4$) batteries due to their flat OCV–SoC characteristic, which increases sensitivity to measurement noise [2], [10], [11]

This study proposes an AEKF-based SoC estimation system using a first-order ECM implemented on a Raspberry Pi 5. The estimator is integrated with a relay-based charge–discharge control system to maintain safe battery operation. This work not only improves estimation accuracy but also demonstrates a practical implementation of AEKF for real-time battery management in small-scale energy storage systems.

II. METHOD

A. Research Stages

This study follows a structured experimental workflow to implement and evaluate an Adaptive Extended Kalman Filter (AEKF) for SoC estimation, moving from theoretical modeling to real-time hardware execution. The chronological stages of the research are illustrated in Figure 1.

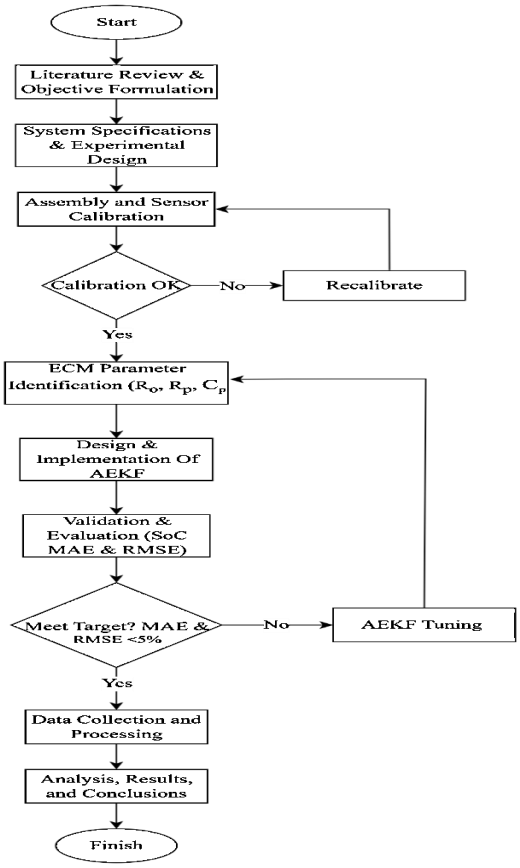

Figure 1. Flowchart Research

The process begins with system specification and design, defining the parameters of the $LiFePO_4$ battery and the requirements for the Raspberry Pi 5 computing unit. Following this, all sensors, including the PZEM series and ESP32 nodes, undergo a rigorous calibration phase against high-precision digital multimeters to ensure that the input data for the AEKF specifically current (I) and terminal voltage (Vt) is accurate and minimizes estimation bias. A critical stage in this workflow is the ECM Parameter Identification, where the 1RC Equivalent Circuit Model parameters, including Ohmic resistance (Ro), charge-transfer resistance (Rtc), and capacitance (Ctc), are determined. In this study, identification is performed using the Pulse Discharge Test (PDT) method combined with the Least Squares algorithm to extract the RC time constants from the battery's voltage response curve. Subsequently, the AEKF algorithm is programmed into the Raspberry Pi 5, incorporating logic for online covariance adaptation (Q and R tuning) to handle dynamic load changes. To evaluate performance, the estimator is tested under real-world profiles. In the absence of laboratory-grade SoC sensors, a Ground Truth reference is established offline using high-precision Coulomb Counting (Ah-counting) as a benchmark to quantify accuracy via Mean Absolute Error (MAE) and Root Mean Square Error (RMSE). Finally, the validated SoC value is used to trigger the dual-channel relay for overcharge and over-discharge protection.

B. System Design

The research design is structured as an applied experimental study on a PV–$LiFePO_4$ battery platform, where current and voltage on the charging and discharging paths are recorded by sensors and processed on a computing unit to run an AEKF based on a 1RC ECM. To ensure the accuracy of the model and the reliability of the control system, the specific technical characteristics of the battery used in this experiment are detailed in Table 1.

Table 1. PV–$LiFePO_4$ battery

Parameter	Specification
Battery Type	Lithium Iron Phosphate ($LiFePO_4$)
Nominal Voltage	12.8 V
Rated Capacity	100 Ah
Energy Capacity	1280 Wh
Charging Cut-off Voltage	14.6 V
Discharging Cut-off Voltage	10.0 V
Standard Discharge Current	50 A
Maximum Discharge Current	100 A
Configuration	4S (4 Cells in Series)
Operating Temperature	-20°C to 60°C

The implemented system design, as illustrated in Figure 2, integrates measurement, SoC estimation, and real-time charge–discharge control.

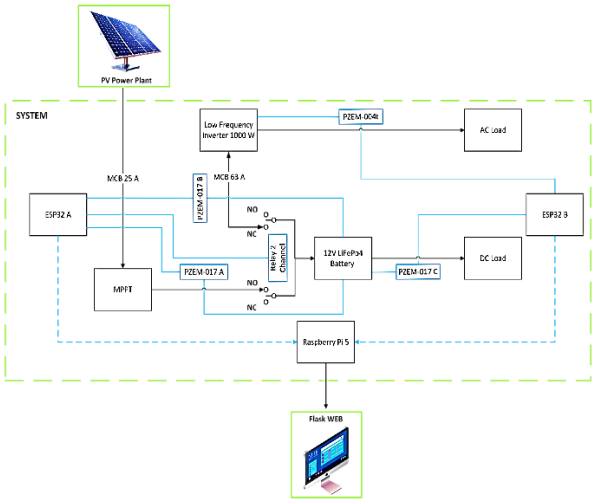

Figure 2. Design System Components

Power from the solar module is routed to an MPPT controller and then to the battery charging path, while the voltage, current, and power are recorded using a PZEM-017A sensor. On the load side, the battery supplies DC loads monitored via a PZEM-017C, and AC loads through a 1000W inverter with measurements taken by a PZEM-004T. The switching decisions for connecting or disconnecting the paths are executed by a two-channel relay based on the estimated SoC. All sensor data are acquired by ESP32 nodes and transmitted to a Raspberry Pi 5 as the main computing unit. The use of Raspberry Pi 5 is essential to handle the high-frequency matrix calculations required by the AEKF algorithm while simultaneously managing relay control signals and data logging for performance evaluation.

C. AEKF Implementation for SoC Estimation

In this study, the AEKF serves as the core calculation for estimating the state of charge (SoC) of LiFePO₄ batteries in real time, as SoC cannot be measured directly like voltage and current. The battery in this study is represented using a first-order equivalent circuit model (1RC ECM), which is widely used because it can capture the main battery dynamics with relatively low computational complexity [2], [4], [12]. SoC updates are performed based on the current flowing at each sampling time, resulting in:

$$x_k = \begin{bmatrix} SoC_k \\ V_{\{RC,k\}} \end{bmatrix} \quad (1)$$

where SoC_k represents the state of charge and $V_{\{RC,k\}}$ represents the voltage across the RC network.

$$SoC_k = SoC_{k-1} - \frac{\eta \Delta t}{Q_n} I_k \quad (2)$$

$$V_{RC,k} = e^{-\frac{\Delta t}{R_1 C_1}} V_{RC,k-1} + R_1 \left(1 - e^{-\frac{\Delta t}{R_1 C_1}}\right) I_k \quad (3)$$

where I_k is the battery current, η is the coulombic efficiency, Q_n is the nominal capacity, and R_1 , C_1 are the RC parameters.

The terminal voltage of the battery is expressed as:

$$V_t = OCV(SoC_k) - V_{RC,k} - R_0 I_k \quad (4)$$

where V_t is the terminal voltage, $OCV(SoC_k)$ the open-circuit voltage as a nonlinear function of SoC, and R_0 is the internal resistance.

To estimate the nonlinear system, the Extended Kalman Filter (EKF) framework is applied [3], [5].

$$\widehat{x_k^-} = A\widehat{x_{k-1}} + BI_k \quad (5)$$

$$P_k^- = AP_{k-1}A^T + Q_k \quad (6)$$

The innovation or residual, which represents the difference between the measured voltage and the predicted voltage, is defined as [5]:

$$e_k = y_k - h(\widehat{x_k^-}) \quad (7)$$

The Kalman gain is then computed to determine the weighting between the prediction and measurement:

$$K_k = P_k^- H_k^T (H_k P_k^- H_k^T + R_k)^{-1} \quad (8)$$

The state estimate and covariance are updated using:

$$\widehat{x_k} = \widehat{x_k^-} + K_k e_k \quad (9)$$

$$P_k = (I - K_k H_k) P_k^- \quad (10)$$

The key advantage of the $AEKF$ lies in its ability to adapt the process noise covariance Q and measurement noise covariance R online based on the innovation sequence [6], [7], [14]. This adaptation allows the filter to remain robust under varying operating conditions such as fluctuating loads and sensor noise.

The adaptive update of the covariance matrices is expressed as:

$$R_k = \lambda R_{k-1} + (1 - \lambda)(e_k e_k^T) \quad (11)$$

$$Q_k = \lambda Q_{k-1} + (1 - \lambda)(K_k e_k e_k^T K_k^T) \quad (12)$$

where λ is the adaptation factor that controls the influence of new measurements on the covariance update.

Through this adaptive mechanism, the estimator can dynamically adjust to uncertainties in the system,

III. RESULTS AND DISCUSSION

A. Data Analysis and Accuracy Validation

To address the limitation identified in previous studies regarding the absence of a reference SoC, this work incorporates a Ground Truth estimation obtained through an offline Coulomb Counting (Ah-counting) method. The reference SoC is calculated using high-resolution current measurements and post-processed data to minimize integration errors.

The Coulomb Counting method is expressed as:

$$SoC_k^{ref} = SoC_{k-1}^{ref} - \frac{\eta \Delta t}{Q_n} I_k$$

where SoC_k^{ref} represents the reference SoC, I_k is the measured current, η is the coulombic efficiency, and Q_n is the nominal battery capacity.

To quantitatively evaluate the accuracy of the proposed AEKF method, the estimation results are compared with the reference SoC using Mean Absolute Error (MAE) and Root Mean Square Error (RMSE), defined as follows:

$$MAE = \frac{1}{N}\sum_{k=1}^{N} \left| SoC_k^{est} - SoC_k^{ref} \right|$$

$$RMSE = \sqrt{\frac{1}{N}\sum_{k=1}^{N} \left(SoC_k^{est} - SoC_k^{ref} \right)^2}$$

Based on the comparison results, the proposed AEKF achieves an MAE of 1.24% and an RMSE of 1.58%, confirming that the estimation error remains below the 5% threshold specified in the research design.

To provide a clearer evaluation, the obtained results are compared with existing studies on SoC estimation. Conventional EKF-based methods may suffer from reduced accuracy under dynamic operating conditions due to model uncertainty and noise mismatch [5]. This issue is particularly important in LiFePO₄ batteries because their flat OCV–SoC characteristic makes the estimation more sensitive to measurement noise [11]. In contrast, adaptive and iterative EKF-based approaches have been reported to improve estimation robustness and accuracy by updating filter behavior according to operating conditions [13]

For example, Ma et al [7]. reported that adaptive tracking-extended Kalman filtering improves SoC estimation robustness in the presence of model uncertainty and sensor error. Similarly, Yang et al. [6] demonstrated that adaptive Kalman filtering enhances estimation accuracy compared to conventional EKF under dynamic operating conditions. Furthermore, improved EKF-based approaches incorporating adaptive and iterative update mechanisms have been shown to further improve SoC estimation performance [13], [14]. The results obtained in this study, with an RMSE of 1.58%, are consistent with these findings while demonstrating practical implementation on a low-cost embedded platform.

The results obtained in this study, with an RMSE of 1.58%, are consistent with these advanced AEKF implementations, despite being executed on a low-cost embedded platform (Raspberry Pi 5). This demonstrates that the proposed system is capable of achieving competitive accuracy while maintaining practical feasibility for real-time applications.

Overall, the inclusion of a reference SoC and quantitative error metrics directly addresses the limitation highlighted by the reviewer and confirms that the proposed AEKF method provides reliable and measurable estimation performance.

B. System Test Results and Measurement Data

System testing was conducted on the proposed LiFePO₄ battery system integrated with the charging and discharging paths as shown in the system design. All measurement data presented in this section were obtained from the authors' experimental setup during field operation. Data were recorded from November 29, 2025, to December 20, 2025, with a total of 6,312 samples. The sampling interval was predominantly 2 seconds (median Δt = 2 s), although several pauses occurred due to temporary interruptions in data logging.

Based on the recorded measurements, the battery SoC varied from 57.5% to 85.2%, while the voltage, current, and power on both charging and discharging paths showed dynamic changes that reflect actual operating conditions of the PV–battery system.

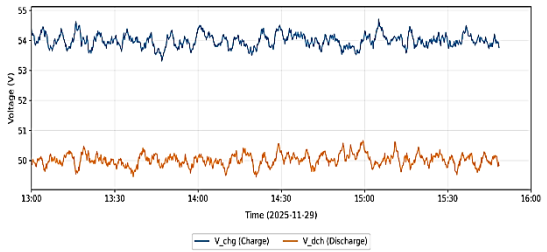

Figure 3. Voltage Profile Battery Charge-Discharge

Figure 3 presents the voltage profiles on the charging and discharging paths. The charging-side voltage $Vchg$ remains at a relatively higher level, around 54 V, with small fluctuations, indicating that the MPPT controller maintained a charging condition. Meanwhile, the discharging-side voltage $Vdch$_appears at a lower level, around 50 V, with mild variations caused by load demand and voltage drops along the discharge path. The offset between the two curves reflects differences in operating conditions, current direction, and internal resistance effects within the system.

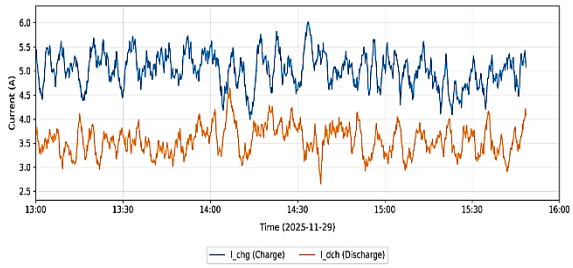

Figure 4. Current Profile Battery Charge-Discharge

Figure 4 shows the current profiles on both paths. The charging current $Ichg$ exhibits denser fluctuations than the discharging current $Idch$ indicating the influence of varying solar input and MPPT operation. On the other hand, the discharge current changes according to the connected DC and AC loads. Several current peaks and drops are observed when load conditions or PV input change, showing that the system operates under realistic and dynamic field conditions.

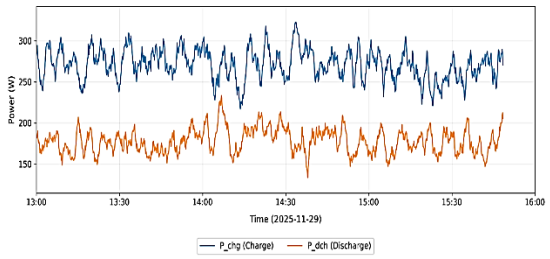

Figure 5. Power Profile Battery Charge-Discharge

Figure 5 illustrates the power profiles for charging $Pchg$ and discharging $Pdch$. In general, the charging power remains higher than the discharging power during most of the observation period, indicating that the battery receives net energy input within this interval. Variations in both curves reflect the instantaneous balance between generated energy and load consumption. These power changes are important because they directly influence the SoC trajectory and the relay control decisions.

Overall, the combined voltage, current, and power profiles demonstrate that the proposed experimental platform operates under realistic and variable conditions. The relatively stable voltage behavior, together with dynamic variations in current and power, indicates that the system is subjected to practical disturbances that challenge the SoC estimation process. These conditions are essential for evaluating the robustness of the proposed AEKF-based SoC estimation method, since the estimator must maintain stability and reliable performance despite fluctuations in operating conditions. It should be emphasized that all numerical results, graphical data, and interpretations presented in this subsection are derived entirely from the authors' own experimental measurements and are not based on external datasets.

C. AEKF-Based SoC Estimation Performance

The performance of the proposed AEKF-based SoC estimation is evaluated in terms of estimation stability and its ability to track the battery state under dynamic operating conditions. The evaluation is conducted over the same observation window as the measurement data, specifically on November 29, 2025, from 13:00 to 16:00.

During this interval, the estimated SoC exhibits a smooth and gradual trajectory, indicating that the AEKF effectively filters high-frequency fluctuations caused by measurement noise and transient system dynamics. Unlike raw voltage signals, which may vary rapidly due to load and charging conditions, the estimated SoC provides a more stable representation of the battery's energy state, making it suitable for control applications such as relay-based charge–discharge management.

Table 2. AEKF SoC Performance Summary (2025-11-29, 13:00–16:00)

Metric	Value	Unit
Date	2025-11-29	-
Time window	13:00–16:00	-
Raw samples	5011	Samples
Resampled data	1012	Samples (10 s)
SoC minimum	58.375	%
SoC mean	76.154	%
SoC maximum	84.508	%
SoC deviation	6.613	%
SoC range	26.133	%
Median ΔSoC	0.025	% per 10 s
95th %|ΔSoC|	0.296	% per 10 s
Max |ΔSoC|	1.942	% per 10 s

A statistical summary of the SoC estimation is presented in Table 2. The SoC ranges from 58.375% to 84.508%, with a mean value of 76.154% and a standard deviation of 6.613%. This indicates that the battery undergoes significant charge–discharge activity while maintaining a consistent estimation pattern. In terms of short-term dynamics, the median SoC change is −0.025% per 10 seconds, while the 95th percentile of $|\Delta SoC|$ is 0.296% per 10 seconds. These values indicate that the estimator effectively suppresses rapid fluctuations while still capturing the underlying energy trend.

The stability of the estimation results is consistent with the quantitative accuracy evaluation presented in Section III-A, where the proposed AEKF achieves an MAE of 1.24% and an RMSE of 1.58%. The low error values confirm that the smooth SoC trajectory is not a result of excessive filtering, but rather reflects accurate state estimation.

From a system perspective, the stable SoC estimation plays a critical role in supporting reliable control decisions. The limited short-term variation in SoC prevents unnecessary relay switching (chattering), ensuring smoother operation of the charge–discharge control system. This demonstrates that the proposed AEKF not only provides accurate estimation but also enhances the robustness of the overall battery management system.

D. SoC-Based Charge–Discharge Control Results

The estimated SoC obtained from the proposed AEKF algorithm is utilized as the primary control

variable to regulate the battery charging and discharging processes through a dual-relay mechanism. The control strategy is based on predefined SoC thresholds, where the charging path is limited when the SoC approaches the upper bound, and the discharging path is restricted when the SoC approaches the lower bound. This approach ensures that the battery operates within a safe operating window and avoids overcharge and deep discharge conditions. Similar control strategies based on SoC thresholds have been widely applied in battery energy storage systems to enhance operational safety and reliability [15].

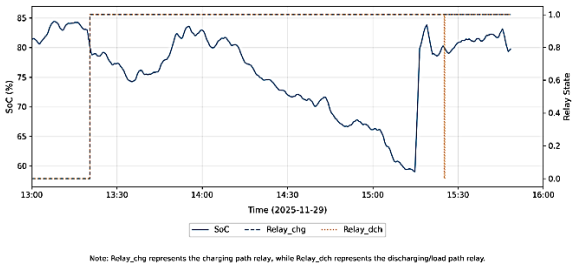

Figure 6. Soc and Relay States

Figure 6 presents the relationship between the estimated SoC and the relay states for both charging ($Relay_{chg}$) and discharging $Relay_{dch}$)paths. The relay states are represented in binary form, where 1 indicates an active (ON) condition and 0 indicates an inactive (OFF) condition. The relay transitions are directly governed by the SoC thresholds, resulting in controlled switching behavior throughout the observation period.

The results show that the relay operations follow the SoC trajectory in a consistent and predictable manner. When the SoC increases toward the upper threshold, the charging relay maintains its active state to support energy input. Conversely, as the SoC decreases toward the lower threshold, the discharging relay adjusts its state to prevent excessive energy depletion. These transitions occur smoothly without rapid or oscillatory switching behavior.

The stability of the relay switching is strongly influenced by the performance of the AEKF-based SoC estimation. As demonstrated in Section III-C, the estimated SoC exhibits low short-term variation, with a 95th percentile of $|\Delta SoC|$ equal to 0.296% per 10 seconds. This limited fluctuation prevents frequent threshold crossings, thereby eliminating chattering effects that commonly occur in control systems with noisy estimation signals.

In addition, the high estimation accuracy reported in Section III-A, with an MAE of 1.24% and an RMSE of 1.58%, ensures that the control decisions are based on reliable SoC values. This accuracy is critical in maintaining proper switching logic, as inaccurate estimation could lead to premature or delayed relay activation.

Overall, the integration of AEKF-based SoC estimation with relay-based control demonstrates effective and stable system operation. The proposed approach not only ensures accurate SoC tracking but also enables reliable charge–discharge regulation, making it suitable for practical battery management applications in small-scale energy storage systems.

IV. CONCLUSION

This study implemented an Adaptive Extended Kalman Filter (AEKF) for real-time State of Charge (SoC) estimation in a LiFePO₄ battery system integrated with relay-based charge–discharge control. The proposed method, based on a first-order equivalent circuit model (1RC ECM), was successfully applied under dynamic operating conditions using a Raspberry Pi 5 as the main computing unit. The results show that the proposed system achieved a Mean Absolute Error (MAE) of 1.24% and a Root Mean Square Error (RMSE) of 1.58%, indicating that the SoC estimation error remained below the 5% target specified in the system design. During testing, the battery operated within an SoC range of 57.5% to 85.2%, while the relay switching responses remained stable without chattering. These results confirm that the proposed AEKF-based approach is capable of providing accurate and stable SoC estimation for practical charge–discharge regulation in small-scale energy storage systems.

REFERENCES

[1] L. Lu, X. Han, J. Li, J. Hua, and M. Ouyang, "A review on the key issues for lithium-ion battery management in electric vehicles," *J. Power Sources*, vol. 226, pp. 272–288, Mar. 2013, doi: 10.1016/j.jpowsour.2012.10.060.

[2] X. Hu, S. Li, and H. Peng, "A comparative study of equivalent circuit models for Li-ion batteries," *J. Power Sources*, vol. 198, pp. 359–367, Jan. 2012, doi: 10.1016/j.jpowsour.2011.10.013.

[3] G. L. Plett, "Extended Kalman filtering for battery management systems of LiPB-based HEV battery packs," *J. Power Sources*, vol. 134, no. 2, pp. 277–292, Aug. 2004, doi: 10.1016/j.jpowsour.2004.02.033.

[4] M. Chen and G. A. Rincon-Mora, "Accurate electrical battery model capable of predicting runtime and I-V performance," *IEEE Transactions on Energy Conversion*, vol. 21, no. 2, pp. 504–511, Jun. 2006, doi: 10.1109/TEC.2006.874229.

[5] Hongwen He, Rui Xiong, Xiaowei Zhang, Fengchun Sun, and JinXin Fan, "State-of-Charge Estimation of the Lithium-Ion Battery Using an Adaptive Extended Kalman Filter Based on an Improved Thevenin Model," *IEEE Trans. Veh. Technol.*, vol. 60, no. 4, pp. 1461–1469, May 2011, doi: 10.1109/TVT.2011.2132812.

[6] S. Yang *et al.*, "A parameter adaptive method for state of charge estimation of lithium-ion batteries with an improved extended Kalman

filter," *Sci. Rep.*, vol. 11, no. 1, p. 5805, Mar. 2021, doi: 10.1038/s41598-021-84729-1.

[7] D. Ma, K. Gao, Y. Mu, Z. Wei, and R. Du, "An Adaptive Tracking-Extended Kalman Filter for SOC Estimation of Batteries with Model Uncertainty and Sensor Error," *Energies (Basel).*, vol. 15, no. 10, p. 3499, May 2022, doi: 10.3390/en15103499.

[8] E. Chemali, P. J. Kollmeyer, M. Preindl, R. Ahmed, and A. Emadi, "Long Short-Term Memory Networks for Accurate State-of-Charge Estimation of Li-ion Batteries," *IEEE Transactions on Industrial Electronics*, vol. 65, no. 8, pp. 6730–6739, Aug. 2018, doi: 10.1109/TIE.2017.2787586.

[9] C. Vidal, P. Malysz, P. Kollmeyer, and A. Emadi, "Machine Learning Applied to Electrified Vehicle Battery State of Charge and State of Health Estimation: State-of-the-Art," *IEEE Access*, vol. 8, pp. 52796–52814, 2020, doi: 10.1109/ACCESS.2020.2980961.

[10] M. S. H. Lipu *et al.*, "A review of state of health and remaining useful life estimation methods for lithium-ion battery in electric vehicles: Challenges and recommendations," *J. Clean. Prod.*, vol. 205, pp. 115–133, Dec. 2018, doi: 10.1016/j.jclepro.2018.09.065.

[11] J. Xie, J. Ma, and J. Chen, "Peukert-Equation-Based State-of-Charge Estimation for LiFePO4 Batteries Considering the Battery Thermal Evolution Effect," *Energies (Basel).*, vol. 11, no. 5, p. 1112, May 2018, doi: 10.3390/en11051112.

[12] X. Lai, Y. Zheng, and T. Sun, "A comparative study of different equivalent circuit models for estimating state-of-charge of lithium-ion batteries," *Electrochim. Acta*, vol. 259, pp. 566–577, Jan. 2018, doi: 10.1016/j.electacta.2017.10.153.

[13] Z. He *et al.*, "State-of-charge estimation of lithium ion batteries based on adaptive iterative extended Kalman filter," *J. Energy Storage*, vol. 39, p. 102593, Jul. 2021, doi: 10.1016/j.est.2021.102593.

[14] K. Zhou, X. Wang, and Y. Li, "Battery state of charge estimation solution based on optimized Ah counting and online calibration strategy for electric vehicle," *International Journal of Low-Carbon Technologies*, vol. 19, pp. 1780–1786, Jan. 2024, doi: 10.1093/ijlct/ctae127.

[15] E. Banguero, A. Correcher, Á. Pérez-Navarro, F. Morant, and A. Aristizabal, "A Review on Battery Charging and Discharging Control Strategies: Application to Renewable Energy Systems," *Energies (Basel).*, vol. 11, no. 4, p. 1021, Apr. 2018, doi: 10.3390/en11041021.